CRREL
REPORT 82-6

**US Army Corps
of Engineers**

Cold Regions Research &
Engineering Laboratory

Measurement of ground dielectric properties using wide-angle reflection and refraction

CRREL Report 82-6

March 1982

Measurement of ground dielectric properties using wide-angle reflection and refraction

Steven A. Arcone and Allan J. Delaney

REPORT DOCUMENTATION PAGE	READ INSTRUCTIONS BEFORE COMPLETING FORM	
1. REPORT NUMBER CRREL Report 82-6	2. GOVT ACCESSION NO.	3. RECIPIENT'S CATALOG NUMBER
4. TITLE (and Subtitle) MEASUREMENT OF GROUND DIELECTRIC PROPERTIES USING WIDE-ANGLE REFLECTION AND REFRACTION		5. TYPE OF REPORT & PERIOD COVERED
		6. PERFORMING ORG. REPORT NUMBER
7. AUTHOR(s) Steven A. Arcone and Allan J. Delaney		8. CONTRACT OR GRANT NUMBER(s)
9. PERFORMING ORGANIZATION NAME AND ADDRESS U.S. Army Cold Regions Research and Engineering Laboratory Hanover, New Hampshire 03755		10. PROGRAM ELEMENT, PROJECT, TASK AREA & WORK UNIT NUMBERS DA Project 4A161102AT24 Task C/E1, Work Unit 005
11. CONTROLLING OFFICE NAME AND ADDRESS Office of the Chief of Engineers Washington, D.C. 20314		12. REPORT DATE March 1982
		13. NUMBER OF PAGES 15
14. MONITORING AGENCY NAME & ADDRESS(If different from Controlling Office)		15. SECURITY CLASS. (of this report) Unclassified
		15a. DECLASSIFICATION/DOWNGRADING SCHEDULE

16. DISTRIBUTION STATEMENT (of this Report)

Approved for public release; distribution unlimited.

17. DISTRIBUTION STATEMENT (of the abstract entered in Block 20, if different from Report)

18. SUPPLEMENTARY NOTES

19. KEY WORDS (Continue on reverse side if necessary and identify by block number)
Cold regions
Geophysics
Radar equipment
Soils
Wave propagation

20. ABSTRACT (Continue on reverse side if necessary and identify by block number)
    The interpretation of continuous radar profiles requires an alternative geophysical means of obtaining ground dielectric information. Ground dielectric properties were measured using wide-angle reflection and refraction (WARR) soundings with a ground-probing radar set that transmits pulses of a few nanoseconds duration. The investigations, carried out over sandy gravel in interior Alaska, provided dielectric data to about a 5-m depth. The WARR soundings were displayed as individual traces allowing interference between separate events and dispersion to be observed, and the soundings were compared with continuous radar and resistivity profiles conducted concurrently to extract the maximum amount of dielectric information. The dielectric constants, derived mainly from the direct ground waves propagating along the surface, ranged from 2.9 to 7.4. Dielectric values interpreted for one site predicted the possibility of a refracted event which may have occurred during one of the soundings.

DD FORM 1473 1 JAN 73 EDITION OF 1 NOV 65 IS OBSOLETE

PREFACE

CONTENTS

ILLUSTRATIONS

MEASUREMENT OF GROUND DIELECTRIC PROPERTIES USING WIDE-ANGLE REFLECTION AND REFRACTION

Steven A. Arcone and Allan J. Delaney

INTRODUCTION

Knowledge of the dielectric properties of soils is essential to the interpretation of ground radar profiling, the calculation of ground reflection coefficients, and the determination of soil water content by airborne remote sensing. In continuous ground radar profiling (Annan and Davis 1976, Davis et al. 1976), the dielectric properties determine signal velocity and are therefore essential to translating echo return times into geologic reflector geometry. Radar profiling is usually carried out at a fixed separation between the transmitting and receiving antennas, while the best method for obtaining dielectric values is to vary the antenna (geophone) separation.

Ground-probing radar has been applied most successfully in the very high frequency (VHF) band of 30 to 300 MHz. At high frequency (3 to 30 MHz) and VHF, horizontally polarized waves have been used to measure ground dielectric permittivity and conductivity by the method known as radio frequency interferometry (RFI) (Annan 1973). In this method, electric properties are calculated from the interference pattern between continously propagating air and ground waves. The method has been used at frequencies as low as 2 MHz (Rossiter et al. 1973) and as high as 88 MHz (Arcone and Delaney 1981).

As offshoot of the RFI method that employs short pulses was discussed by Annan and Davis (1976). In this technique, known as WARR (wide-angle reflection and refraction), the time delays between air ground wave pulses are measured to determine dielectric properties. Annan and Davis used a ground-probing radar, the antennas of which were continuously separated. They recorded their results on strip chart forms where the horizontal axis was antenna separation and the vertical axis the time of propagation. The slope of the first signal received after the air wave then gave them a good measure of the ground surface dielectric constant.

An example of a continuous WARR profile is shown in Figure 1. The dark bands represent signal amplitude and the thin, light bands are zero voltage levels in the return signals. The various sloping profiles correspond to a variety of propagation modes (discussed in the next section). In this type of display, information that could be derived from the waveforms, such as dispersion, interference and phase reversals, is not available.

In this report the ability of the WARR technique to evaluate dielectric properties is thoroughly examined by displaying the individual waveforms at several discrete antenna separations as in seismic work. The soundings are compared with continuous radar reflection profiles at fixed antenna separation and also with low frequency resistivity profiles in order to extract the maximum amount of dielectric information. For the WARR soundings, the antennas were separated in 1.0-m intervals to 14 or 15 m to investigate the top 4 to 5 m of low loss sands and gravels at three sites in interior Alaska.
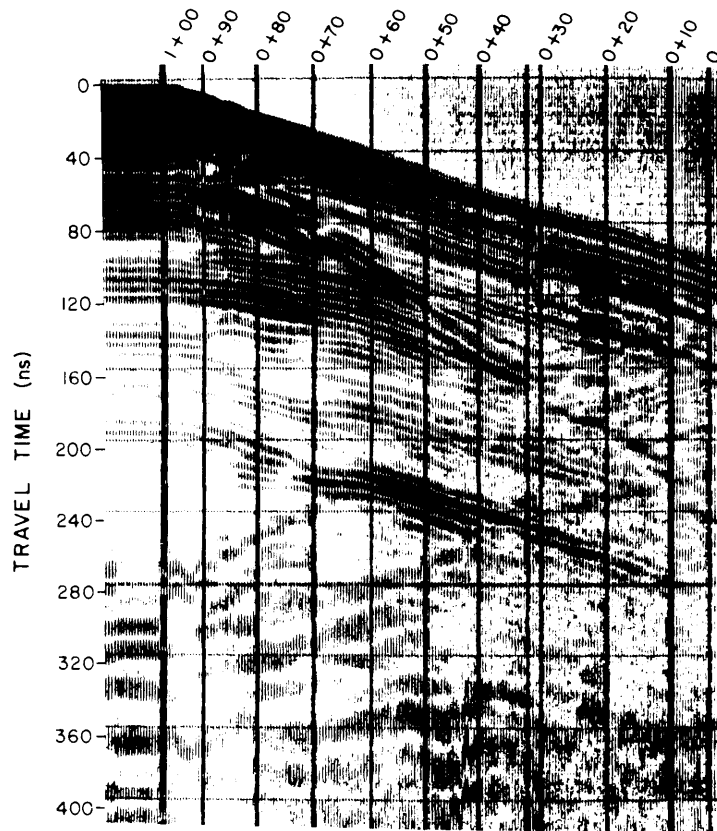
Figure 1. Example of a continuous WARR profile (from Annan and Davis 1976). The horizontal axis is antenna separation in feet. The darkness (paper burn) depends on signal intensity.

THEORY OF GROUND WAVE PROPAGATION FROM A HORIZONTAL ELECTRIC DIPOLE

The theory of wave propagation in the steady state from a horizontal electric dipole lying on or near the earth's surface has been well treated by Kong (1972), Annan (1973), Annan et al. (1975) and Chlamtac and Abramovici (1981) as well as by many others. These discussions provide a good basis for understanding pulse propagation in homogeneous ground because pulses may be synthesized from an infinite number of plane wave trains. In layered ground, however, this approach will not apply because, with continuous radiation, waveguide modes exist that are not analogous to the events observed with pulses.

Figure 2 (from Annan 1973) presents the four modes that are excited when a horizontal electric dipole is placed on the surface of a homogeneous model earth. The modes are referenced to a right-hand Cartesian coordinate system, x, y,

z. In the figure, wavefront A represents a spherical air wave above the surface, and wave B represents a spherical wave excited in the ground. Waves C and D propagate above and below the ground, respectively, in order to maintain the continuity of the tangential electric and magnetic fields of waves B and A across the air/ground interface. Wave C, the ground surface wave, is termed "inhomogeneous" in that it attenuates exponentially with height above the surface. It propagates with the same horizontal phase velocity as B. Wave D is called a head wave and it propagates with the same horizontal phase velocity as A. The RFI technique is based on the interference between waves C and A, while the WARR technique is based on their separation in time.

The velocity of wave propagation in the ground is much slower than in air. Consequently, in order for A to match D at the air/ground interface, wave D must propagate at an angle β such
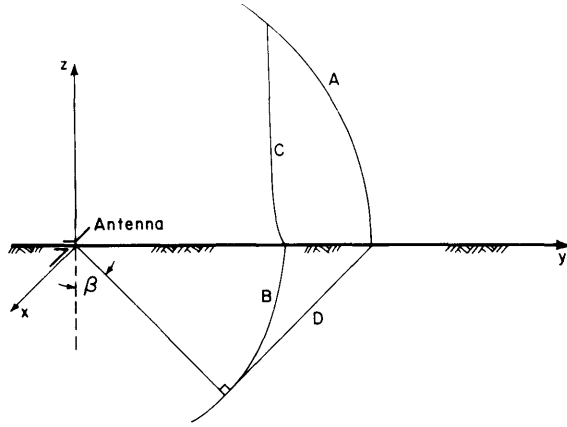
2

Figure 2. Various modes radiated in the broad-side direction from a horizontal electric dipole lying on the surface of a homogeneous earth (from Annan 1973). The modes are described in the text. The angle $\beta = \sin^{-1}(k_0/k_1)$.
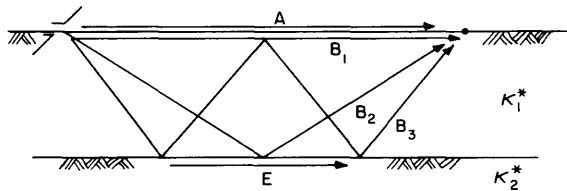

Figure 3. Possible reflection and refraction events in a two-layer ground. A is the air wave, B_1 the ground surface wave, B_2 and B_3 reflections from the subsurface interface and E a refracted wave which will occur if $\kappa_2 > \kappa_1$.

that $\sin \beta = k_0/k_1$ where k_0 and k_1 are the propagation functions in air and ground, respectively. These functions are given by

$$k_0 = \sqrt{\omega^2 \mu_0 \varepsilon_0} \tag{1}$$

and

$$k_1 = \sqrt{\omega^2 \mu_0 \kappa^* \varepsilon_0 + i\omega\mu_0/\varrho} \tag{2}$$

where κ^* is the relative complex dielectric permittivity, which may be expressed as

$$\kappa^* = \kappa' + i\kappa''. \tag{3}$$

κ' is usually termed the dielectric constant and κ'' the loss factor. In these expressions ω is frequency in rad/s, $\mu_0 = 4\pi \times 10^{-7}$ H/m, $\varepsilon_0 = 8.85 \times 10^{-12}$ F/m, ϱ is resistivity in ohm-m, $i = \sqrt{-1}$ and the time dependence $e^{-i\omega t}$ has been as-

sumed. The loss tangent of a medium is defined as

$$\tan \delta = (\kappa'' + 1/\varrho\omega\varepsilon_0)/\kappa'. \tag{4}$$

In air the phase velocity of wave A is simply the phase velocity c of light in a vacuum. The phase velocity of wave C is ω/k_1 which for $\tan \delta \ll 1$, equals $c/\sqrt{\kappa'_1}$.

The addition of a subsurface interface creates several additional events as illustrated by the rays in Figure 3. The layering produces a waveguide effect and gives a $1/\sqrt{y}$ dependency to the amplitudes of the guided, subsurface reflection, in contrast to the $1/y^2$ dependency for the ground surface wave. Of course, the initial amplitudes of all the multiple reflections will be reduced from that of the ground surface wave. If a layer is sufficiently thin there will also be a low frequency filtering effect on the pulse, but this was not encountered in these studies. Also shown in Figure 3 is the possibility that a refracted wave will occur if $\kappa^*_2 < \kappa^*_1$.

EQUIPMENT AND METHODS

The equipment used for this investigation was a Geophysical Survey Systems Inc. radar system, featuring a model 4000 mainframe, model 700P control module and model 76 transmitting and receiving antennas. The antennas (resistively loaded, bowtie-type dipoles) were in two separate housings. The transmitting antenna emits a pulse of several nanoseconds duration, and the received signals are sampled and converted to an audio frequency facsimile for display. The time scale can be determined from a supplied, calibrated oscillator or by physically separating the antennas a known distance and calibrating the time delay, as was done for this investigation.

Figure 4a shows the shape of the pulse emitted when the antenna radiates into space. This pulse shape was obtained by placing the antennas over a perfectly conducting plane and separating them several free-space wavelengths of the pulse center frequency (1.0 m). At closer distances, the received pulse was a synthesis of direct, indirect (i.e. reflected) and ground waves. By about 3 m, however, the direct and indirect waves had canceled each other and only an air surface wave, which has the same time dependency as a free space wave, remained. The duration of one cycle of this far-field pulse shape is about 3.3 ns, giving a center frequency to the Fourier spectrum of about 300 MHz.

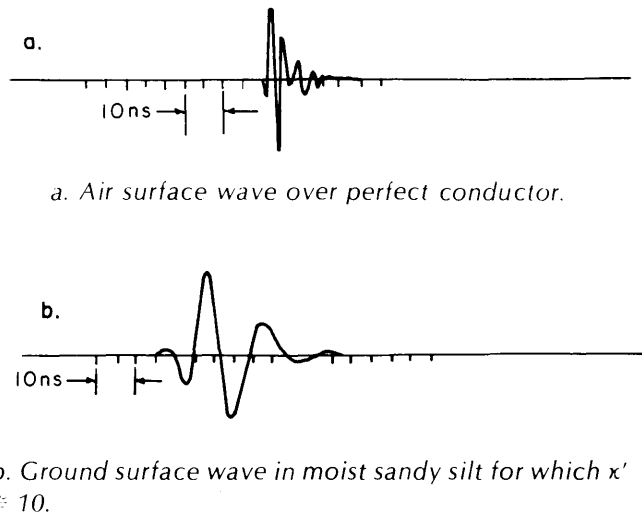Figure 4b shows the alteration of this pulse

3

a. Air surface wave over perfect conductor.

b. Ground surface wave in moist sandy silt for which x'
≈ 10.

Figure 4. Far-field radar pulse shapes.

shape when the antennas are coupled to ground. In this case the antennas are separated over a sandy silt with a dielectric constant of about 10.0. The frequency content of this ground surface wave over the perfect conductor and the relative amplitudes between the peaks have changed.

The theoretical difference in time delay between the air wave signals propagating over antenna separations of 1 and 14 m was used to check the calibration of an internally generated time scale for all positions. The internal time calibration was always within ±1.5 ns of the theoretical difference of 43.33 ns. The time delays of reflection and refraction events were measured from an internally recorded "start of scan" pulse which initiated every scan of the pulse returns. The returns were recorded in an "A-scope" (amplitude vs time) type of display.

Two different antenna positions, both producing horizontal polarization and broadside radiation, were used for the WARR profiling at each site. One was the normal profiling position for which the antennas were designed. This position places the plane of the "bowtie" of the antenna parallel with the ground and gives the best ground coupling, but produces an air wave of very small amplitude because a metal shield is attached behind the antenna. The other position simply has the bowtie turned on its broadside edge. This position gives poor ground coupling but the air wave is strongly launched.

To verify the presence of any suspected layering, continuous radar profiles were performed along each sounding line of the WARR measurements using a different antenna set (transmitter and receiver separated by 30 cm) housed in one unit. Low frequency resistivity measurements were also made to verify the dielectric nature of the ground. The resistivity measurements were performed with a magnetic induction device (Geonics EM-31), the theory and operation of which may be found in Arcone et al. (1979) and Arcone and Delaney (1981). The device uses two loop antennas separated by 3.66 m and can employ them in two different orientations that allow approximate penetration depths of 3 and 6 m. Increases in d.c. resistivity were interpreted as indicative of decreasing water content and vice versa. This interpretation implies a corresponding decrease in dielectric constant at VHF with increasing resistivity.

RESULTS

Site 1

This site is part of a glacial outwash plain of sand, silt and gravel located at Ft. Greely, Alaska, and now used infrequently as an airfield. The area is flat and the organic cover has been cleared. Immediately below the surface are numerous fossil ice wedge casts filled with silt. The horizontal beds of stratified sand and gravel about the casts are generally distorted towards the vertical. Church et al. (1965) have documented many cross sections of these casts. A perched water table exists at about 10 m.
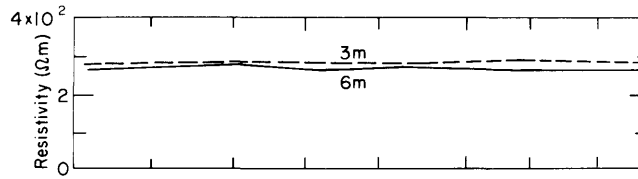
a. Low frequency magnetic induction resistivity profile
for penetration depths of 3 and 6 m.
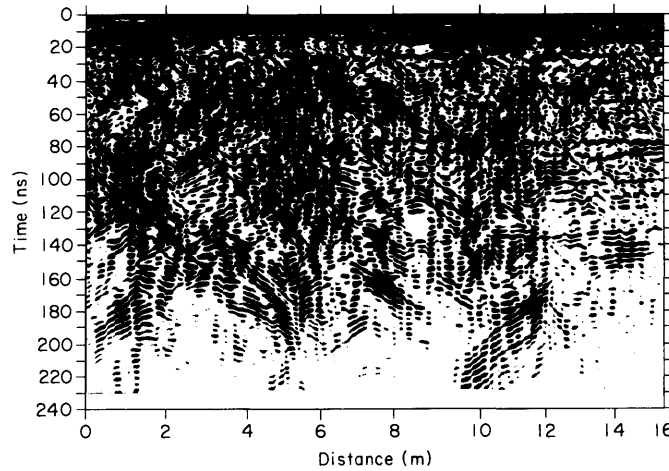
b. Radar profile.

Figure 5. Continuous radar reflection and low frequency
magnetic induction resistivity profiles along an 18-m
traverse at Ft. Greely.

Figure 5 shows the continuous radar and resistivity profiles along an 18-m segment of the airfield. The resistivity profile shows a surprising lack of variation both vertically and horizontally, but the dielectric contrast between the silt in the casts and the sand and gravel causes the complexity of the radar profile. These strong returns mainly show multiple hyperbolas caused by scattering from the localized casts. Further discussion of this and continuous radar profiles from this site will be presented in Arcone et al. (1982).

Figure 6 shows the individual WARR traces taken across the profile. The transmitting antenna was situated at the 0-m station of Figure 5 and the receiving antenna at stations 1-15. Times at which the events of strongest amplitude align from trace to trace are connected by straight lines and replotted in Figure 7. The slopes of these plots allow the signal velocity to be calculated and, hence, also the corresponding dielectric constant. The plot at the top of Figure 7 is for the air wave, and the data points for this plot were taken from a separate WARR spread with the antennas oriented on edge for better air wave coupling. The intersection of the air wave plot with the vertical axis gives the correct zero time reference.

The slope of each plot gives a dielectric constant of about 5.5. Since x' for dry sand or gravel can be as low as 2.6, some moisture was in the ground, as also shown by the low resistivity values. The later events shown in Figure 7 are believed to have scattered from a silt-filled cast in the vicinity of the transmitter (0 m) and are revealed by the wide hyperbola starting downward at about 0 and 2 m at 20 ns in Figure 5. If these plots were of multiple reflections from a layer interface, then their slopes would have appeared to be merging asymptotically.

These WARR dielectric results give the same implication of homogeneity as the resistivity profile, probably because both were integrating electrical responses that occurred over horizontal and vertical distances that were greater than those of the casts (approximately 1-2 m). The
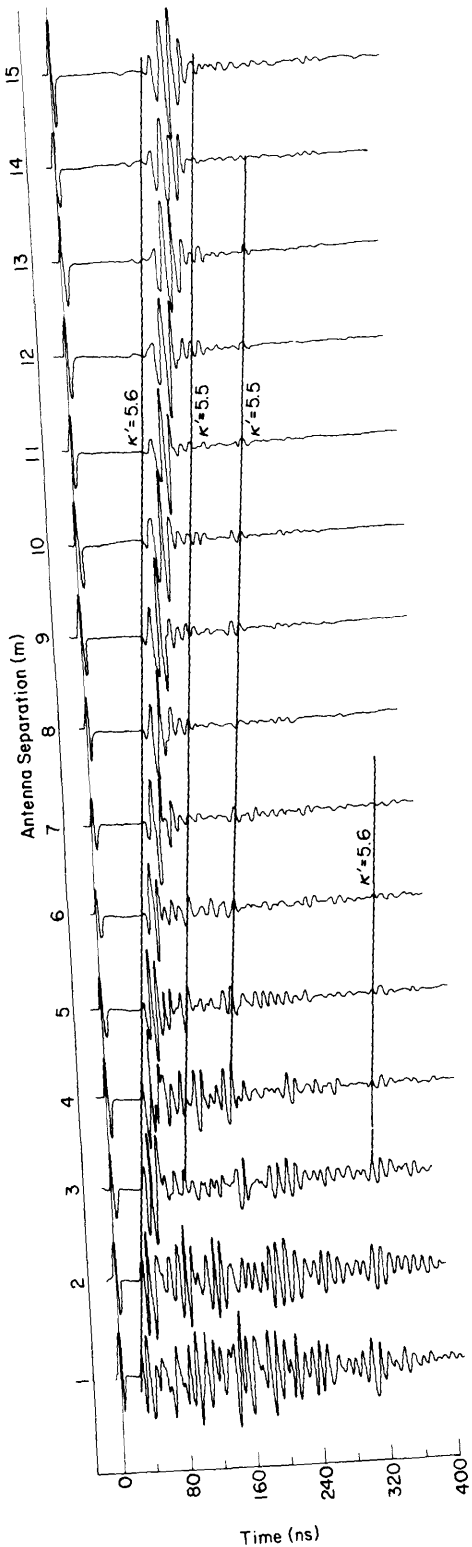
Figure 6. WARR sounding at Ft. Greely. The first pulse at 0 ns is artificially generated to start the scan and serves as a time reference.
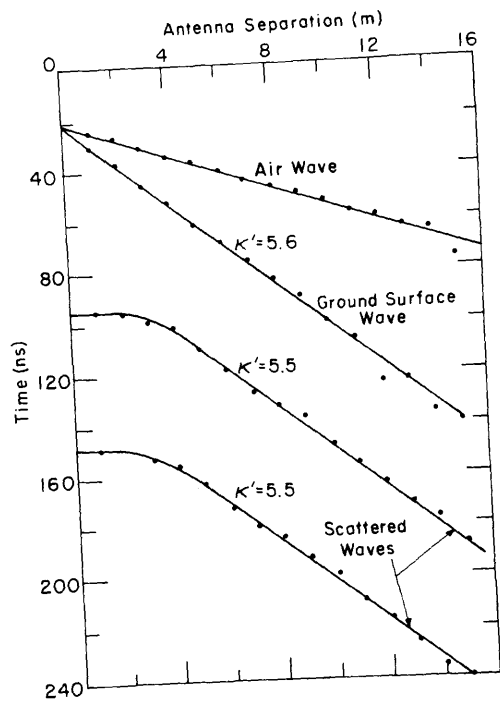

Figure 7. Time-distance plots taken from some of the events observed in Figure 6.

continuous radar profile, however, does not integrate over large distances so that greater detail was revealed.

Site 2

This site is located at Ft. Wainwright in Fairbanks, Alaska, and is part of the Tanana River floodplain. The site material is mainly silt, sand and gravel, with most of the silt having been bladed off to form a road. The silt is 5.1 m above the Chena River which was within 100 m. Therefore the water table is at a depth of approximately 5.1 m.

Figure 8 shows the continuous radar and resistivity profiles along a 14-m section of the road. The second layer occurs at a delay of 35 to 40 ns and is probably the base of the frozen material. The third layer seems to occur at a delay of about 65 ns and presents a more diffused return. This event is assumed to be the water table. The resistivity profile gives much higher values than at site 1 and shows resistivity to be increasing with depth. This increase may be due to greater amounts of coarse-grained material at depth or to a decrease in moisture content down to the water table, as might be caused by upward moisture migration during freezing. Unfrozen adsorbed water is presumed to cause the lowest resistivities near the surface.
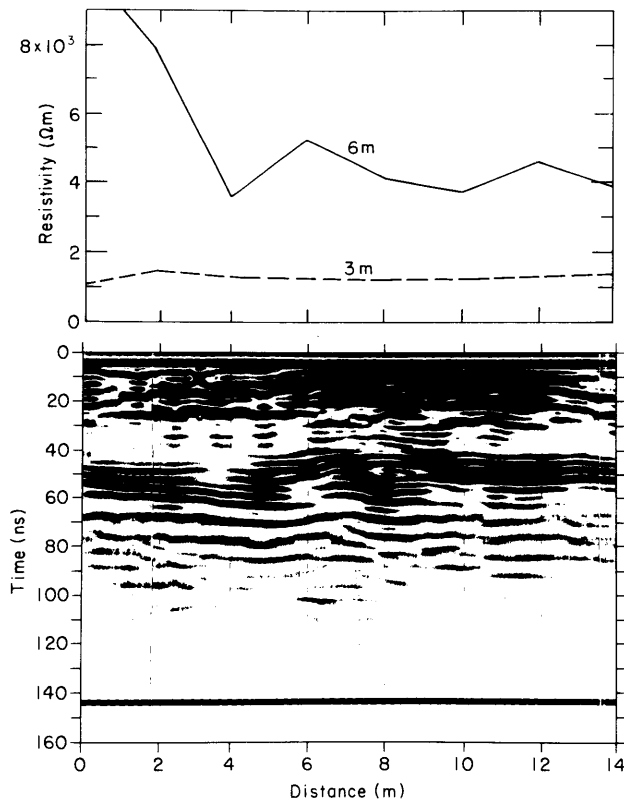
6

Figure 8. Continuous radar reflection and low frequency magnetic induction resistivity profiles along a 14-m traverse at Ft. Wainwright (bladed road site).

Figures 9 and 10 show the individual WARR sounding traces (transmitter at 0 m) and the corresponding time-distance plots for several of the events. The air wave shown here and the ground surface wave do not intercept the time axis at the exact same point because the antennas were in the normal profiling position, which does not allow good air-wave coupling. The other plots show a very characteristic two-layer behavior with the slopes all merging at large distances. As it is impossible to pick out the leading edge of each multiple event, the depth of the first layer interface is estimated to be about 2.5 m and the dielectric constant of this first layer is calculated from the slopes of the plots to be about 4.8.

Since the water table is at 5.1-m depth, the second layer is about 2.6-m thick. The second layer return is about 30 ns behind the first layer return in Figure 8 so that the dielectric constant of the second layer is calculated at about 3.0 using the formula $x' = (ct/2d)^2$ where d is layer depth, c is free space velocity and t is round-trip time of propagation within the layer. This value is con-

sistent with the above hypothesis of a drier material as deduced from the resistivity data. This value also implies that a refracted wave may occur along the interface between layers 1 and 2, as the second layer is calculated to be of a higher velocity medium than the first.

This analysis provides the subsurface model for site 2 shown in Figure 11. Also shown in Figure 11 is a ray path for a refracted ray which should exist for this model. The angle of incidence upon the first subsurface interface for the refracted ray is $\sin^{-1} \sqrt{x'_2/x'_1} = 52.2°$. The first antenna station to receive this refracted ray would be at 7.0 m, as the refraction first reaches the surface at the theoretical distance of about 6.5 m. At the 7-m station, the refracted wave should be about 15 ns behind and in phase with the ground surface wave. An event thought to be this refraction occurs at the 7-m station in Figure 9. The exact phase agreement between this event and the ground surface wave is not evident since the pulses overlap. The ground surface and refracted waves should then cross over (in phase with no time displacement) at the 15-m
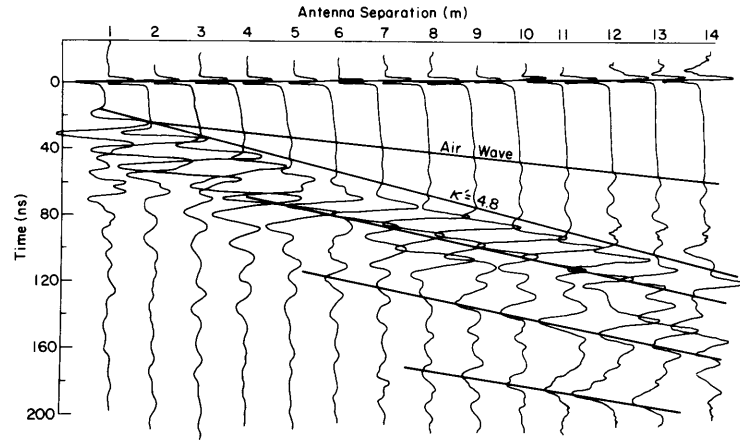
7

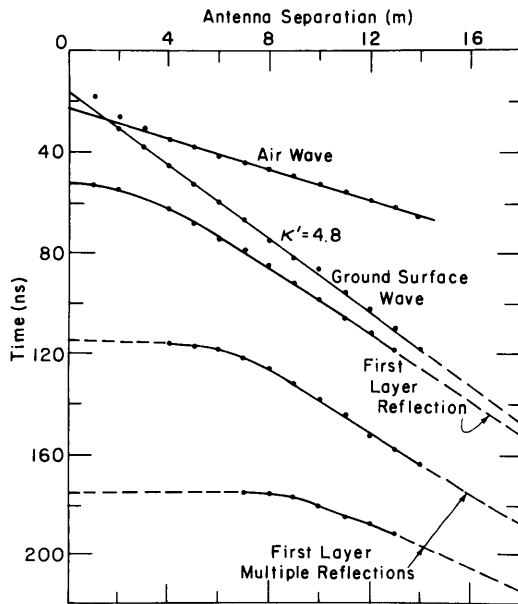Figure 9. Radar WARR sounding, Ft. Wainwright (bladed road site).

Figure 10. Time–distance plots taken from events observed in Figure 8.

station. At the 14-m station the theoretical time delay difference is 4 ns (or just slightly less than one-half the period of the pulse) and, in fact, serious distortion of the leading edge of the ground surface wave occurs here.

Site 3

This site, also located at Ft. Wainwright, is in the same area as site 2 and of the same kind of gravelly sand. The area has been used as a gravel pit. No visible evidence of the water table was present in nearby pits but it is known to be more than 5 m deep.

Figure 12 shows the continuous radar and resistivity profiles along a 14-m section of the area. The radar profile shows a possible two-layer structure between 0 and 8 m and then some uninterpretable returns between 8 and 14 m. The resistivity profiles show that the near-surface resistivity more than doubles across the section while the deeper values generally stay between 600 and 900 ohm-m.

The individual WARR sounding traces in Figure 13 also show a severe disturbance in electrical structure beginning at 7 m. More data could have been collected to resolve this structure, but the primary purpose was to measure dielectric properties. In Figure 14 the earliest returns give a dielectric constant of 2.9, which implies a very dry surface layer of sand or gravel. The low value is most usually associated with resistivity values at 10^4 ohm-m or above. A secondary wavelet gives a dielectric value of 7.4 out to a distance of 9 m before this return is interfered with by the returns from the inhomogeneity. The wavelet traveling at $\kappa' = 2.9$ is the ground surface wave, whereas the wavelet traveling at $\kappa' = 7.4$ is probably the part of the ground surface wave wavefront that has been continuously refracted downwards and reflected from the interface shown at about 35 ns in Figure 12. Within this layer the dielectric constant probably increases continuously with depth. If 7.4 is about the average dielectric constant for the layer, then a time delay of about 35 ns gives a layer depth of about 1.9 m.
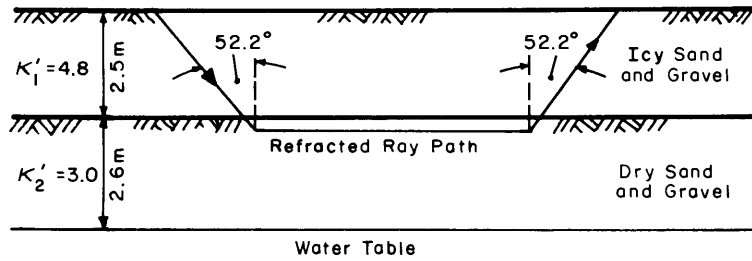
8

Figure 11. Subsurface model for site 2 based on the WARR and continuous radar profiling data. The surface elevation of the site above the nearby Chena River was used for the water table depth of 5.1 m, the WARR data were used for calculating $\kappa_1 = 4.8$ and the first layer depth of 2.5 m, and the continuous radar reflection profile was used to calculate $\kappa_2 = 3.0$.
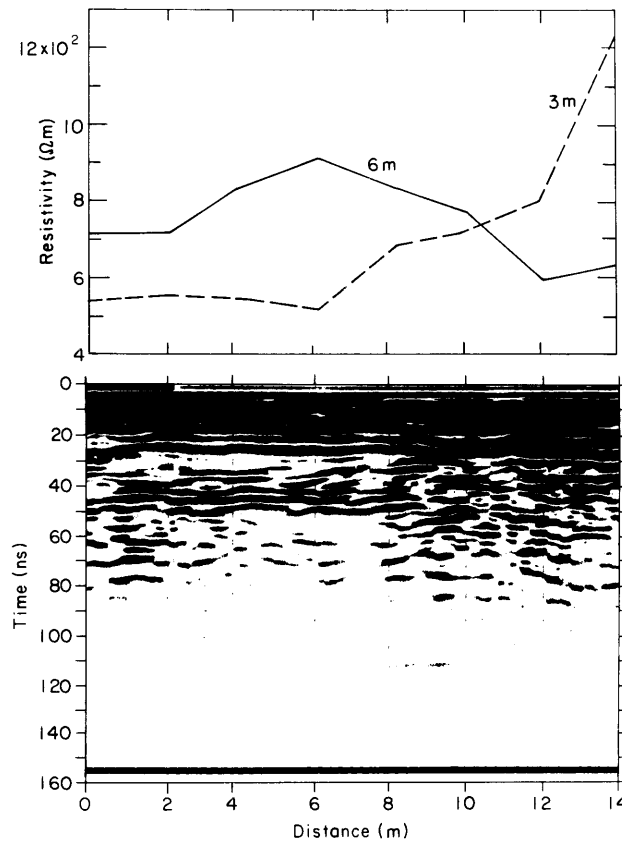

Figure 12. Continuous radar reflection and low frequency magnetic induction resistivity profiles along 14-m traverse at site 3 (Ft. Wainwright gravel pit site).

SUMMARY AND CONCLUDING REMARKS

These investigations have shown that WARR soundings are an effective aid to radar profiling because of the dielectric information they provide. At site 1 the κ' value of 5.5 obtained for the sand and gravels was shown to be an effective bulk value over the few meters of depth of the silt ice wedge casts. At site 2 the combination of WARR, continuous profiling and knowledge of the water table allowed the dielectric permittivity of two separate layers to be evaluated. At site 3, the WARR soundings revealed that the bulk
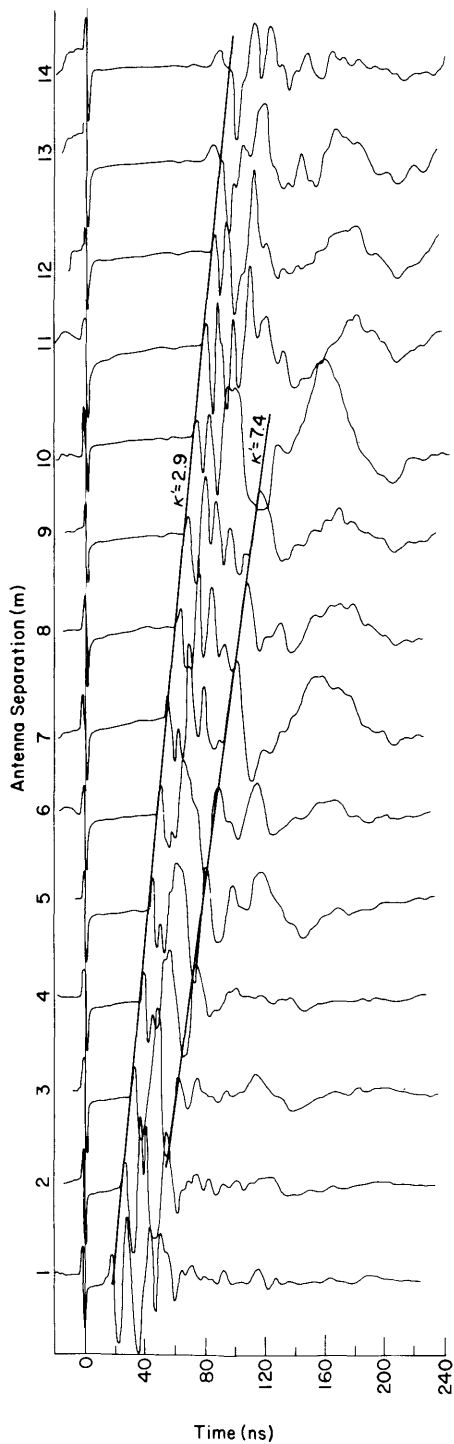
9

Figure 14. Time-distance plots taken from events observed in Figure 12.

Figure 13. Radar WARR sounding, Ft. Wainwright (gravel pit site).

permittivity value of the upper few meters of ground was not the same as the surface value so that permittivity was increasing with depth.

At all three sites the ground surface was flat so that the antennas were in close ground contact and no elevation corrections had to be applied to the traces. If the antennas had been elevated by any surface roughness or by a snowpack, the ground surface wave events would have been seriously attenuated. This is because the amplitude dependency on height above ground for a horizontally polarized ground surface wave is proportional to exp $[-(k_1^2 - k_0^2)^{1/2} z]$ where z is height. At the value $\kappa' = 5$, this attenuation rate works out to be about 0.25 dB/cm at a frequency of 80 MHz.

The dielectric properties of soils show little dispersion for small water contents (i.e. less than 5% by volume), as was shown by the uniformity of shapes seen from trace to trace in Figures 6, 9 and 13 for the ground surface waves. Although the relative amplitudes of the peaks changed slightly, the period of oscillation remained fairly constant throughout the sounding. Dispersion is associated with high loss tangents. The highest possible loss tangent that may have been encountered would have been at the Ft. Greely airstrip where, for a d.c. resistivity of about 300 ohm-m and a wavelet center frequency of 80 MHz, the loss tangent (eq 4) would have been moderate at about 0.13. However, in this case the ground surface waveforms were consistently uniform with little dispersion.

10

The main advantage of continuous WARR pro-filing is that reference points within the subsur-face returns may be easily traced to allow the calculation of dielectric constants and layer depths. When used in the discrete mode, the waveform display allows dispersion, interfer-ence and phase changes to be identified. In addi-tion, good antenna-ground coupling need only be maintained at discrete stations. Finally it should be mentioned that, in the discrete mode, signal enhancement techniques such as stacking and deconvolution can be applied most easily.

LITERATURE CITED

Annan, A.P. (1973) Radio inteferometry depth sounding: Part I. Theoretical discussion. *Geophy-sics*, vol. 8, no. 3, p. 557–580

Annan, A.P., W.M. Waller, D.W. Strangway, J.R. Rossiter, J.D. Redman, and R.D. Watts (1975) The electromagnetic response of a low-loss, 2-layer dielectric earth for horizontal electric dipole ex-citation. *Geophysics*, vol. 40, no. 2, p. 285–298.

Annan, A.P. and J.L. Davis (1976) Impulse radar sounding in permafrost. *Radio Science*, vol. 11, no. 4, p. 383–394.

Arcone, S.A., A.J. Delaney and P.V. Sellmann (1979) Effects of seasonal changes and ground ice on electromagnetic surveys of permafrost. CRREL Report 79-23, ADA077903.

Arcone, S.A. and A.J. Delaney (1981) Electrical properties of frozen ground at VHF near Pt. Bar-row, Alaska. CRREL Report 81-13.

Arcone, S.A., P.V. Sellmann and A.J. Delaney (1982) Radar detection of ice wedges. CRREL Re-port (in prep).

Chlamtac, M. and F. Abramovici (1981) The elec-tromagnetic fields of a horizontal dipole over a vertically inhomogeneous and anisotropic earth. *Geophysics*, vol. 46, no. 6, p. 904–915.

Church, R.E., T.L. Péwé and M.J. Andersen (1965) Origin and environmental significance of large-scale patterned ground: Donnelly Dome area, Alaska. CRREL Research Report 159, ADXL-474477.

Davis, J.L., W.J. Scott, R.M. Morey and A.P. An-nan (1976) Impulse radar experiments on perma-frost near Tuktoyaktuk, Northwest Territories. *Canadian Journal of Earth Sciences*, vol. 13, p. 1584–1590.

Kong, J.A. (1972) Electromagnetic fields due to dipole antennas over stratified anisotropic me-dia. *Geophysics*, vol. 37, no. 6, p. 985–996.

Rossiter, J.R., G.A. LaToracca, A.P. Annan, D.W. Strangway, and G. Simmons (1973) Radio inter-ferometry depth sounding: Part II. Experimental results. *Geophysics*, vol. 38, no. 3, p. 581–599.